Hindawi
Mathematical Problems in Engineering
Volume 2022, Article ID 8130609, 11 pages
https://doi.org/10.1155/2022/8130609

Research Article

A Digital Assessment Method for Multisource Influence Factors on Corrosion Characteristics in the Karst Areas

Zhanfei Gu [1,2,3] **and Zhikui Liu** [1,3]

[1]*College of Civil Engineering and Architecture, Guilin University of Technology, Guilin, Guangxi 541004, China*
[2]*College of Civil Engineering and Architecture, Zhengzhou University of Aeronautics, Zhengzhou, Henan 450046, China*
[3]*Technical Innovation Center of Mine Geological Environmental Restoration Engineering in Southern Area, Nanning, Guangxi 530029, China*

Correspondence should be addressed to Zhikui Liu; 1998009@glut.edu.cn

Received 11 June 2022; Revised 9 July 2022; Accepted 13 July 2022; Published 25 August 2022

Academic Editor: Punit Gupta

Taking dolomite and limestone in Guilin and Liuzhou regions in the north of Guangxi Province as research objects, this paper analyzed their mineral composition and chemical composition and proposed a digital assessment method for multi-source factors on corrosion characteristics in the Karst areas. Specifically, the chemical corrosion test, the corrosion test under the chemical-temperature actions, and the corrosion test under the action of vibration load are carried out from the digital view, respectively. Four aspects can be found in digital assessment results. Firstly, the dolomite in northern Guangxi mainly has a fine crystalline texture and a massive structure with low content of acid-insoluble matters, while limestone mainly has a powder crystalline texture and a massive structure with high content of acid-insoluble matters, and the purity of both dolomite and limestone are very high. Secondly, the difference of corrosion between dolomite and limestone mainly depends on the ratio of CaO/MgO in their chemical composition and the content of silica and acid insoluble matters. Thirdly, the corrosion rates of pure dolomite and pure limestone are basically the same under the same external conditions. Finally, temperature and vibration load have a relatively large influence on the corrosion rates of dolomite and limestone, and the corrosion rates of dolomite and limestone increase with the increase of temperature, but the influence of vibration load on the corrosion rate is more significant than temperature. This research can provide theoretical basis and technical support for large-scale engineering construction and prevention of karst geologic disasters in karst stone mountainous areas in northern Guangxi.

1. Introduction

In carbonate rock areas, due to the differences in mineral composition and chemical composition of rock mass, the differences in internal structure and pore characteristics, and the influence of external conditions such as groundwater occurrence, temperature, and vibration load, dolomite and limestone distributed in these areas have differential corrosions. The differential corrosions often destroy the integrity of the rock mass, affect the mechanical properties and stability of the rock mass, and have a great impact on the safety of buildings and constructs attached to it. China's karst landforms are widely distributed with a large area, and mainly distributed in Guangxi, Guizhou, and eastern Yunnan. It is one of the largest karst areas in the world, with large continuous limestones and dolomites distributed. With the continuous reinforcement of China's economic strength and the continuous advancement of the development strategy in Southwest China, the strategic planning of "Silk Road Economic Belt" and "twenty-first Century Maritime Silk Road," urban railway transits, underground utility tunnels, and other infrastructure constructions have achieved unprecedented development, and numerous large-scale infrastructures such as high-speed railways and

highways have been started in Southwest China one after another. Due to the complexity of geological structure in Southwest China, engineering geological problems have appeared in most projects, among which karst geologic disasters are overriding. The wide range of karst distribution has seriously hindered the development of transportation infrastructure in Southwest China. Therefore, it is of great engineering practical significance to profoundly study the structural characteristics and differential corrosions of the limestone and dolomite.

The research on karst geologic disasters is mainly divided into two categories: theoretical research on corrosion mechanisms and research on karst detection methods. The corrosion test of carbonate rocks is an important content of theoretical research. Scholars in the past have done a lot of experiments on the corrosion characteristics of carbonate rocks, and have achieved many results. Liu et al. [1] used the two-scale continuous medium model to simulate the dissolution reaction process and predict the optimal injection rate during acidification treatment of carbonate rocks and put forward a general numerical method to simulate structured and unstructured reaction flow problems. Zhao et al. [2, 3] proposed a new alternative method for theoretically dealing with the evolution process of chemical dissolution surface in water-saturated porous rocks when propagating in a chemical system. In this method, porosity, pore fluid velocity, and acid concentration were taken as independent variables so that the problem of water-rock interaction could be solved by numerical methods and algorithms. Liu et al. [4] studied the infiltration and corrosion change process of carbonate rocks under different dynamic water pressure conditions, and the results showed that the infiltration and corrosion along the internal pores of rocks had an important influence on corrosion rate. Liu [5] and Gu [6] analyzed the characteristics of carbonate rocks from macro- and micro-perspectives, focusing on the investigation of the influence of differential weathering of limestones and dolomites on the causes of avalanche, stone peaks, and rocky desertification. She et al. [7] studied the morphology of carbonate rocks after corrosion by scanning electron microscope (SEM), and found that although the mineral composition and content of carbonate rocks have a certain influence on their corrosion, the types and connectivity of pores formed after the corrosion are more closely related to the formation of favorable carbonate rock reservoirs. Wei et al. [8, 9] studied the corrosion of rocks containing dolomitic limestone and dolomitic limestones from different corrosion time scales. Under the same pH value and the same corrosion time, the corrosion rate of dolomitic limestones is higher than that of rocks containing dolomitic limestone. Zhang et al. [10] revealed that the rock microstructure plays a controlling role in the corrosion rate, and the corrosion rates of dolomites with different structures are as follows: mesocrystalline to fine crystalline dolomites > fine crystalline to powder crystalline dolomites > powder crystalline to micritic dolomites; the specific surface area is related to the total corrosion amount, but independent of the corrosion rate per unit surface area. The corrosion starts from intergranular and intercrystalline pores, structural microfractures, and cleavage, and gradually expanded to make pores and fissures connected with each other. The abovementioned pieces of research on corrosion investigated the corrosion characteristics of limestones and dolomites from the aspect of the water-rock interaction mechanism with the consideration of the influence of lithology, the characteristics of acidic solution and microorganisms, etc., which provides a theoretical basis and practical reference for the research of this project. On the basis of the above research results, taking the action factors of temperature and vibration load into account can further confirm and improve the above research conclusions and would be more in line with the actual situation, so it has certain feasibility and important significance.

Temperature is one of the important factors affecting the mechanical properties of rocks. Rock is composed of solid mineral particles and tiny gaps between the particles. The solid mineral particles and the channel networks formed by gaps between the mineral particles are often filled with fluid media. When changes in the environment of such porous media of rocks occur, the water presenting in the pores and fissures inside the rocks will undergo a phase change, leading to changes in the physical and mechanical properties of the rocks. These changes are not only related to their physical structure but also affected by the existing water, temperature, and stress state in the rocks. A lot of research have been done on this influence at home and abroad. She et al. [11] found that with the increase in temperature, the dissolution amount of carbonate rocks showed the pattern of slow decline-slow rise-rapid decline, of which 80–100°C is a favorable temperature. Nomeli et al. [12] used a kinetic model extended based on the standard Arrhenius equation to study the corrosion rate of calcite in the temperature range of 50–100°C and the pressure up to 600 bar and determined the functional relationship between calcite dissolution and temperature, pressure, and salinity. Eliwa et al. [13] studied the thermodynamics and kinetics of the dissolution process of carbonate rocks. Mutlutuk et al. [13] found that the change in temperature can destroy the rock integrity through repeated cyclic freeze-thaw experiments, and the more times and higher frequency of freeze-thaw cycles are undergone, the greater the loss of rock integrity occurs, and the more obvious the characteristics of damage and destruction is. Ding et al. [14] took the limestone from Longmen Grottoes in Luoyang as the research object and carried out mechanical tests under the action of different hydrochemical solutions and freeze-thaw coupling with the consideration of the influence of the erosion of limestone seepage solution and freeze-thaw damage in winter. Yang et al. [15] used diamond anvil cell (DAC) technology to conduct corrosion experiments and concluded that with the increase in stratum temperature and pressure, limestone exhibits obvious cementation (sediment), and dolomite is not more easily corroded than limestone under the conditions of acidic stratum fluid with a high temperature and high pressure. Temperature is an important factor that affects the dynamic mechanical properties of rocks and the internal structure of rocks will

be damaged due to temperature changes. After undergoing temperature changes, the strength and deformation of rocks have great changes, which will have a great impact on engineering structures.

Under the action of vibration load and stress, the primary pores, crack propagation, and fracture of carbonate rocks will change the permeability, and the carbonate rocks show different characteristics in different stress-strain stages. Xie et al. [16] studied the ground vibration under the coupling action of earthquake and high-speed trains. The coupling of the two will increase the dynamic displacement of the ground. When the speed of the train is greater than a certain critical value, the coupling effect is significant. Vital et al. [17] studied the hydrodynamic problems in the concretion and dissolution processes of carbonate rocks in the southeast Buenos Aires Province, Argentina, and pointed out the influence of mineral particle size on hydrochemistry and the relationship between mineral structure changes and hydrodynamic pressure in the process of dissolution. Ma et al. [18] carried out tests on seepage characteristics of fissuring rock masses under different confining pressures. The groundwater transported in rock cracks is affected by the width of cracks and their interconnection, and is also strictly controlled by the geometric shape and confining pressure conditions required by water flow. Ishibashi et al. [19] discussed the seepage evolution of cracks in carbonate rocks caused by mechanical stress and nonequilibrium chemistry (pH value). According to the combination of constraint stress and liquid pH, pore spaces of cracks are either open (permeability increases) or closed (permeability decreases). Sheng et al. [20] through designing experiments under different working conditions and with the condition of changing osmotic pressure and chemical solutions, acquired the change of fissure permeability under the action of stress, and theoretically described the permeability characteristics of rock mass fissures under the seepage-stress-chemical coupling action, and further revealed the mechanism of the seepage-stress-chemical coupling action. Chen et al. [21] reviewed the research status of thermal, water, and mechanical properties of rock masses under low temperature and freeze-thaw cycle conditions, and put forward to establish a water-heat coupling model of rock masses with phase transition at low temperature and a turbulence model of tunnel airflow field by considering the influence of air temperature and humidity by the means of field monitoring, a large number of indoor freeze-thaw tests, and uniaxial and triaxial compression tests. Chen [22, 23] reviewed the impact of vibration caused by train operation on the foundation based on the field test data.

To sum up, there are many kinds of research focusing on the corrosion of dolomite and limestone under the action of chemistry, temperature, and vibration load, but the existing chemical corrosions and researches in karst areas mainly focus on limestone-dominated areas or areas with miscellaneous lithology, so the study on corrosion in areas with dolomite-dominated lithology needs to be further strengthened. Scientific problems such as differential corrosion characteristics of rocks and identification of influencing factors in dolomite and limestone development areas have not been completely solved. Therefore, it is of great theoretical and practical significance to systematically carry out tests to determine the structural characteristics and differential corrosions of limestone and dolomite and explore the influencing mechanism of differences between dolomite and limestone in karst geologic disasters.

2. Test Samples

2.1. Collection and Analysis of the Test Samples. Several limestone and dolomite samples were collected from large-scale construction sites such as highways, main roads, and urban railway transits in the Guilin and Liuzhou regions in the north of Guangxi. After returning to the laboratory, the representative samples were selected and analyzed for the minerals and structural characteristics of the rocks with an optical microscope, so as to roughly obtain the mineral composition, structural characteristics, and name of the samples. The specific test results are shown in Table 1.

2.2. Description of Characteristics of the Test Samples. In the process of mineral and rock identification, it is difficult to accurately judge the mineral and rock only by naked eyes and simple tools for some fine-grained, micro-grained, aphanitic, or vitreous rocks; so it is necessary to triturate the 0.03 mm thick rock or mineral slices and identify with the aid of an optical microscope. The transmission polarizing microscope is used for the identification of transparent minerals, while the reflection polarizing microscope is used for the identification of opaque minerals. The test samples shown in Table 1 are photographed with an optical microscope and further described in details below.

2.2.1. Test sample No. 1. The rock has a fine crystalline texture. The rock is composed of 0.06–0.25 mm dolomite. The dolomite is in irregular particles with a poor automorphic degree, and the particles are closely embedded into aggregates (Figure 1). The dolomite is not colored with the alizarin red staining. The rock contains 2% calcite, 97% dolomite, and $<$ 1% others.

2.2.2. Test sample No. 2. The rock has a fine crystalline texture. The rock is mainly composed of 0.03–0.06 mm calcite and a small amount of carbonaceous and siliceous minerals (Figure 2). The rock contains 85% calcite, 8% carbonaceous mineral, and 7% siliceous mineral. The calcite is colored with the alizarin red staining, and its content is about 85%. The rock minerals are slightly oriented.

2.2.3. Test sample No. 3. The rock has a fine crystalline texture. The rock is composed of 0.06–0.25 mm dolomite. The dolomite is in irregular particles with poor automorphic degree (rhombus is found locally). The particles are closely embedded into aggregates (Figure 3). The dolomite is not colored with the alizarin red staining. The rock contains 98% dolomite and 2% calcite.

Table 1: Mineral composition and structural characteristics of the test samples.

Sample no.	Macroscopic observation	Mineral composition	Structure construction	Name
1	The rock is in gray-white color, with a fine crystalline texture and massive structure. It bubbles slightly when dropping cold diluted HCl solution. It is mainly composed of carbonate minerals.	Dolomite: 97%; calcite: 2%; others: 1%	Fine crystalline texture, massive structure	Fine-grained dolomite
2	The rock is in dark black color, with a powder crystalline texture and massive structure. The rock is so hard that a knife cannot strike on it. The rock is in dark black, but it does not pollute the hands. It bubbles strongly when dropping cold diluted HCl solution. It is mainly composed of carbonate minerals, carbonaceous matter, and siliceous matter.	Calcite: 85%; carbonaceous matter: 8%; siliceous matter: 7%	Powder crystalline texture, massive structure	Carbonaceous siliceous limestone
3	The rock is in gray-white color, with a fine crystalline texture and massive structure. It bubbles slightly when dropping cold diluted HCl solution. It is mainly composed of carbonate minerals.	Dolomite: 98%; calcite: 2%	Fine crystalline texture, massive structure	Fine-grained dolomite
4	The rock is in gray color, with an argillaceous texture and massive structure. The knife can strike on it. The rock powder has a slippery feeling. It is mainly composed of mud. It is in lamina and lamellation configuration. The minerals have a slightly oriented arrangement, but not obvious. A thin layer of pyrite is found in the hand specimen, which is granular aggregates and concentratedly distributed locally.	Dolomite: 98%; calcite: 2%.	Argillaceous texture, massive structure	Pyrite-bearing and sand-bearing mudstone
5	The rock is in gray color, with a powder crystalline to mesocrystalline texture and massive structure. It bubbles strongly when dropping cold diluted HCl solution. It is mainly composed of carbonate minerals. It fragments in a later stage, with broken cracks in lattices interspersed.	Calcite: 98%; dolomite: 1%; others: 1%	Powder crystalline to mesocrystalline texture, massive structure	Mesocrystalline limestone
6	The rock is in gray-white color, with a fine crystalline texture and massive structure. It bubbles slightly when dropping cold diluted HCl solution. It is mainly composed of carbonate minerals.	Dolomite: 97%; calcite: 2%; others: 1%	Fine crystalline texture, massive structure	Fine-grained dolomite
7	The rock is in dark gray color, with a mesocrystalline texture and massive structure. It bubbles weakly when dropping cold diluted HCl solution. It is mainly composed of carbonate minerals. The rock is broken, with broken cracks interspersed.	Dolomite: 98%; calcite: 2%	Mesocrystalline texture, massive structure	Mesocrystalline dolomite
8	The rock is in black color, with a microcrystalline to powder crystalline texture and massive structure. It bubbles slightly when dropping cold diluted HCl solution. It is mainly composed of carbonate minerals and carbonaceous matter.	Dolomite: 40%; calcite: 55%; carbonaceous matter: 5%	Microcrystalline to powder crystalline texture, massive structure.	Carbonaceous dolomite

2.2.4. Test sample No. 4. The rock has an argillaceous texture. The rock is mainly composed of clay minerals, a small amount of quartz sand, and a small amount of granular pyrite. The rock contains about 90% clay minerals, about 5% quartz sand, and about 5%pyrite, with quartz sand and pyrite scattered (Figure 4). Sandy grains vary from 0.05 to 0.20 mm and are mostly subround. Pyrite is opaque (Figure 5), with a size of 0.02–0.04 mm. Minerals are in an oriented arrangement, but not obvious.

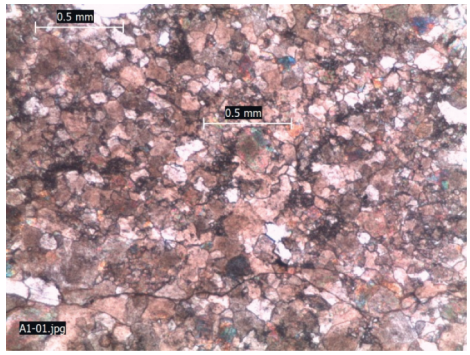

Figure 1: Fine-grained dolomite.

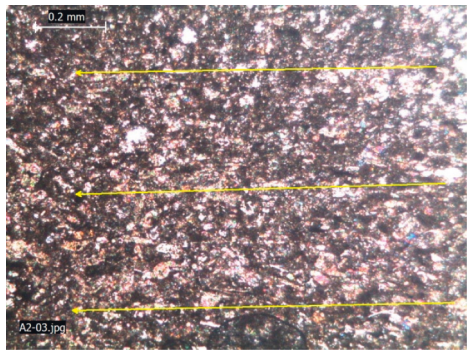

Figure 2: Carbonaceous siliceous limestone.

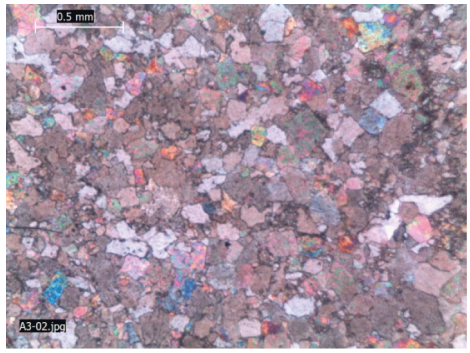

Figure 3: Fine-grained dolomite.

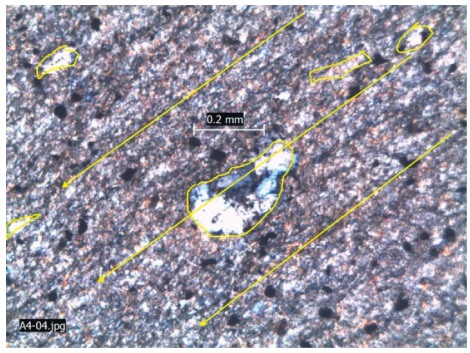

Figure 4: Pyrite and sand-bearing mudstone.

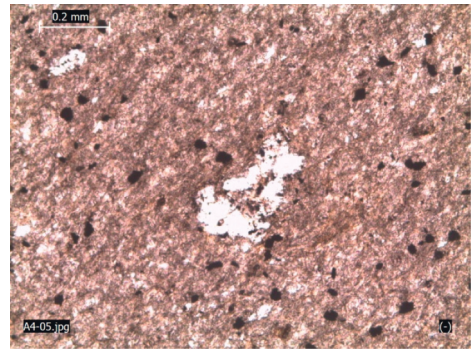

Figure 5: Pyrite and sand-bearing mudstone.

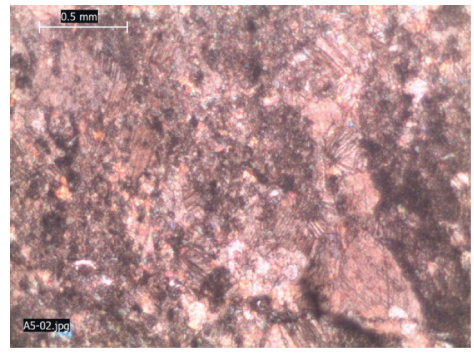

Figure 6: Mesocrystalline limestone.

2.2.5. Test sample No. 5. The rock has a powder crystalline to the mesocrystalline texture (Figure 6). The rock is mainly composed of 0.03–0.50 mm calcite minerals. The calcite is irregularly granular, in rhombohedron, rhombic cleavage, high-grade white interference color, and 0.03–0.50 mm in size, of which over 80% is in the range of 0.25–0.50 mm. The calcite is red and the dolomite is not colored when the rock is dyed with alizarin red. The rock contains 98% calcite, 1% dolomite, and < 1% other organic matters. In the later stage, the broken cracks are interspersed and filled with calcite (Figure 7).

2.2.6. Test sample No. 6. The rock has a fine crystalline texture. The rock is composed of 0.05–0.25 mm dolomite, of which more than 95% is in the range of 0.06–0.25 mm. The dolomite is in irregular particles with a poor automorphic degree. The particles are closely embedded into aggregates (Figure 8). The dolomite is not colored with the alizarin red staining. The rock contains 2%, 97% dolomite, and < 1% others. In the later stage, the cracks are filled with calcite.

2.2.7. Test sample No. 7. The rock has a fine crystalline and mesocrystalline texture. The rock is mainly composed of 0.05–0.50 mm dolomite minerals (Figures 9 and 10), of which 15% is in the range of 0.05–0.25 mm and 85% is in the range of 0.25–0.50 mm. Only the calcite filled in the cracks is colored with the alizarin red staining, with a content of about 2% (Figure 10). The remaining is mainly dolomite with a content of about 98%.

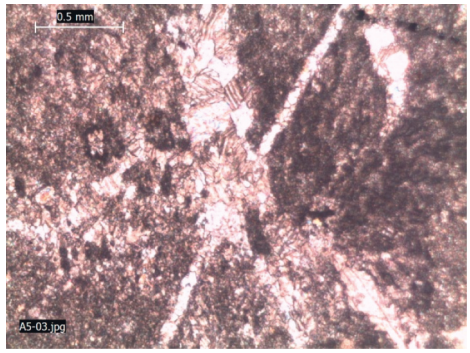

Figure 7: Mesocrystalline limestone.

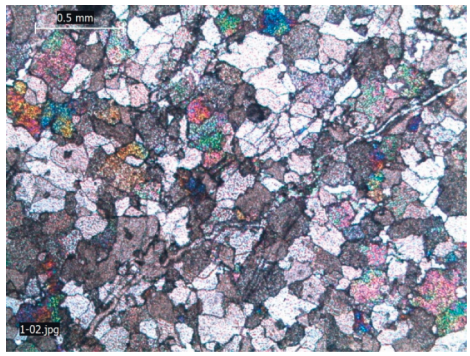

Figure 8: Fine-grained dolomite.

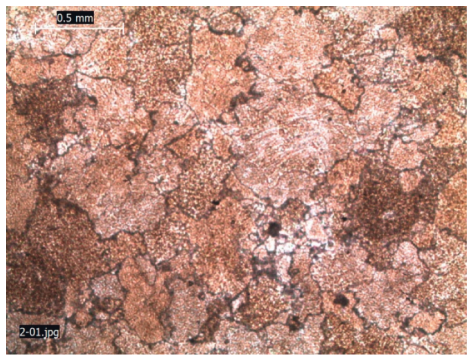

Figure 9: Mesocrystalline dolomite.

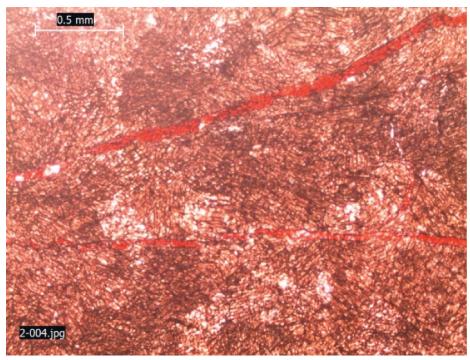

Figure 10: Mesocrystalline dolomite.

2.2.8. Test sample No. 8. The rock has a microcrystalline to powder crystalline texture and is mainly composed of dolomite, calcite, and opaque carbonaceous mineral. The mineral particle size is mainly between 0.005 and 0.10 mm, of which more than 70% is in the range of 0.03–0.06 mm. The rock is dyed with alizarin red and contains about 40% calcite, about 55% dolomite, and 5% carbonaceous mineral and others (Figures 11 and 12). The calcite is irregularly granular, with high-grade white interference color, and is evenly distributed in the rock. The dolomite is irregularly granular, with a particle size of 0.05–0.10 mm.

2.3. Chemical Composition Analysis of the Test Samples. As shown in Table 1, the above description that the test samples taken in the experiments are mainly crystalline dolomites and limestones with high purity (except for test sample no. 4). The test samples with good appearance and characters other than test sample no. 4 were select, and detected for the amounts of CaO, MgO, CO_2, SiO_2, acid insoluble matter, and loss on ignition by using the high-frequency infrared sulfur-carbon analyzer and X-ray fluorescence spectrometer, respectively. The specific test results are shown in Table 2. Then the ratio of CaO/MgO was calculated to judge the purity of dolomite and limestone [24, 25]. Among them, dolomite and limestone with high purity were selected, and then the subsequent corrosion tests were carried out.

3. Corrosion Tests

The corrosion (corrodibility) of water is an internal factor of water-rock interaction, and the mobilization property and chemical characteristics of water will inevitably affect the characteristics of action of water on carbonate rocks. The main acidic fluids of dolomite and limestone corrosion in the actual field environment are the aqueous solutions of CO_2, organic acids, and H_2S. However, in the indoor simulation tests, the acidity of the carbonic acid solution is weak, and its reaction with limestone and dolomite is slow under static conditions. When calcium chloride or solution containing calcium ions is added to the aqueous solution of organic acids, insoluble calcium salt precipitate can be formed. H_2S gas is toxic. In acidic solutions commonly used in laboratories, SO_4^{2-} in sulfuric acid solution will react with the corroded Ca^{2+} and Mg^{2+} to generate slightly soluble substances and insoluble substances, which will affect the determination of Ca^{2+} and Mg^{2+}. At the same time, due to the fairly long reaction process between the ions in groundwater and the minerals in rocks in nature, it is difficult to obtain ideal test results under limited time and conditions, so hydrochloric acid solution at pH 3.0 was specially prepared for the indoor accelerated corrosion tests.

3.1. Comparison of the Static Corrosion Test Results between Dolomite and Limestone under the Same Conditions. All the devices used in this experiment are self-designed, and the experimental devices mainly include a thermostat, vibration equipment, pH measuring instrument, measuring

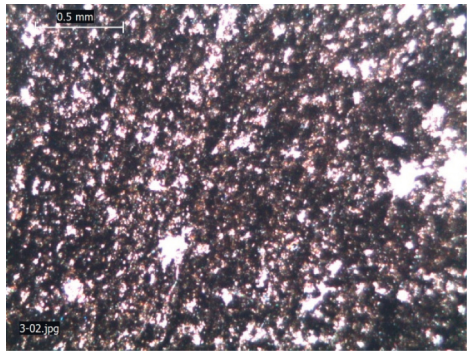

Figure 11: Carbonaceous dolomite.

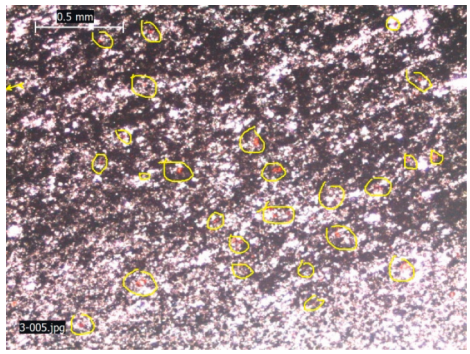

Figure 12: Carbonaceous dolomite.

equipment for Ca^{2+} and Mg^{2+}, and related chemicals and reagents, etc. The thermostat and temperature controller can keep the experimental environment at a stable temperature all the time and reduce the influence caused by the external environment. A constant speed stirrer is mounted at the bottom of the thermostat, which makes the solution flow through the rotation at a constant speed, thus simulating the outdoor hydrodynamic conditions.

In order to reduce the discreteness of the test samples, the rock samples taken for the experiment were made into cylindrical slices, and the pulsed ultrasonic penetration method was used to detect and screen the samples, from-which the rock samples with similar wave velocities were selected. The specific experimental steps are as follows:

(i) Measuring the diameter and height of the rock samples by vernier caliper and weighing the rock samples (Table 3), and calculating the parameters such as surface area, volume, and density;

(ii) Washing the test samples with distilled water, drying them in an oven, cooling them in a dryer to room temperature and weighing;

(iii) Adding 5 L hydrochloric acid solution at pH 3.0 into a clean beaker, and adding the rock samples successively;

(iv) Standing at room temperature, removing the corroded liquid every 2 hours, and measuring the concentration of calcium and magnesium ions in the solution by ethylene diamine tetraacetic acid (EDTA) solution titration method;

(v) Determine the pH of the remaining solution, and calculate the corrosion amount of the rock samples. In order to eliminate the influence of surface area differences of the rock samples, the results of this experiment are expressed by the corrosion amount per unit of surface area.

As shown in Figure 13, the corrosion rates of dolomite and limestone are basically the same under static conditions, and the corrosion amount per unit surface area for dolomite is 0.341 mg (average value), which is slightly larger than that of limestone (0.328 mg). And there is little difference between them for a long time.

3.2. Comparison of Dolomite Test Results under Different Conditions. Temperature is one of the important factors affecting the mechanical properties of rocks. Rock is composed of solid mineral particles and tiny gaps between the mineral particles. The solid mineral particles and the channel networks formed by the gaps between the mineral particles are often filled with fluid media. When the environment of such porous media of the rock changes, the water existing in the pores and fissures inside the rock would undergo a phase change, which leads to changes in the physical and mechanical properties of the rock. These changes are not only related to the physical structure but also affected by the existing water, temperature, and stress state of the rock. At the same time, under the action of vibration load and stress, the primary pores, crack propagation, and fracture of dolomite and limestone cause the permeability to change, and then the dolomite and limestone exhibit different characteristics in different stress-strain stages. In order to study the influence of temperature and vibration load on the corrosions of dolomite and limestone, a group of dolomite and limestone were specially selected (the specifications and size of the samples are shown in Table 4), and the corrosion tests were carried out at different temperatures (0°C and 40°C) and vibration conditions. The corrosion results of the selected samples under different conditions are shown in Table 4 and Figure 14. Vibration conditions: The authors fixed a crossbar on the upper part of the Electric Sieve Shaker(the vibration amplitude is 10 mm, and the number of shocks is about 150 times/min.), and then use a thin cotton thread to tie the rock sample to one end of the crossbar. The sample is shaken every half an hour for 2 to 3 minutes.

As shown in Figure 14, the corrosion rate of dolomite is the lowest at 0°C, and is increased at 40°C, but the difference is not significant. However, the corrosion rate and amount of dolomite are increased significantly under the vibration condition, and the corrosion rate under the vibration condition is about 1.75 times of the corrosion rate at 0°C. The results indicate that vibration load has a more significant effect on the corrosion rate of dolomite than temperature.

As shown in Figure 15, the corrosion rate of limestone is the lowest at 0°C, the corrosion amount is increased at 40°C, and the variation amplitude of limestone is larger than that of dolomite. At the same time, the corrosion rate and amount of limestone under the vibration load are also increased significantly, and the corrosion rate under the

Table 2: List of chemical composition analysis of dolomite and limestone test samples.

Sample no.	Field naming	Chemical composition of dolomite and limestone samples (%)						
		CaO	MgO	SiO_2	Loss	Acid insoluble matter	CO_2	CaO/MgO
1	Dolomite	36.07	16.78	0.27	45.96	0.48	45.13	2.15
2	Limestone	36.20	3.25	15.17	33.29	23.74	31.57	11.13
3	Limestone	50.32	4.51	0.64	43.10	1.31	42.71	11.16
4	Limestone	53.65	0.39	0.90	42.79	1.72	42.52	137.56
5	Limestone	20.38	2.55	32.03	22.15	53.08	18.21	7.98
6	Dolomite	32.14	20.27	0.24	46.15	0.31	45.76	1.59
7	Dolomite	32.14	20.27	1.18	46.05	2.68	45.65	1.59
8	Dolomite	32.07	19.95	1.32	45.93	2.60	45.34	1.61
9	Limestone	29.91	2.74	26.93	28.00	37.72	26.01	10.90

Table 3: List of parameters and corrosion results of limestone and dolomite test samples.

Sample no.	Lithology	Weight g	Diameter mm	Height mm	Surface area mm^2	Volume mm^3	Density g/cm^3	Corrosion amount mg	Corrosion amount per unit area, mg/mm^2
1–14	Dolomite	120.81	68.87	12.21	10087.07	45461.68	2.66	3583.01	0.355
3–6	Dolomite	115.27	69.25	11.54	10038.35	43442.52	2.65	3473.27	0.327
2–10	Limestone	127.23	70.58	12.69	10633.39	49624.32	2.56	3293.24	0.328

vibration load is about 1.88 times of the corrosion rate at 0°C. The results demonstrate that the corrosion rate of limestone is highly sensitive to both temperature and vibration load.

4. Analysis and Discussion of the Test Results

The corrosion of erosive aqueous solution is an internal factor of water-rock interaction, and the mobilization property and chemical characteristics of water affect the characteristics of action of erosive aqueous solution on dolomite and limestone. With the progress of water-rock interaction, the change of internal structure and pore characteristics of rock would inevitably lead to the unceasing change of groundwater seepage field. At the same time, the hydrochemical property in the rock mass also changes correspondingly, which is mainly reflected in the coupling process of the chemical field, temperature field, and stress field of water-rock interaction.

The dolomite (from Liuzhou area) selected in this study has a CaO/MgO ratio of less than 2.2, an acid insoluble content between 0.31% and 0.68%, and a SiO_2 content between 0.24% and 1.32%, so it belongs to pure dolomite. The selected limestone (from the Guilin area) has a CaO/MgO ratio of greater than 10, the contents of acid insoluble matter and SiO_2 are generally higher, and the purity is slightly lower. In pure carbonate rocks, the corrosion rate of calcite is generally higher than that of dolomite, and the corrosion rate increases with the increase of calcite content and decrease with the increase of dolomite content. In the impure carbonate rocks, due to the increase of acid insoluble matters and SiO_2 content, the amount of physical damage is increased, which inhibits the relationship between the corrosion rate and the calcite and dolomite content. Similarly, the structure of rock also has a certain influence on the corrosion rate. Generally speaking, the smaller the grain size, the larger the specific surface area, and the faster the corrosion rate. Therefore, in this study, the corrosion rates of dolomite and limestone are basically the same under the same conditions. However, under the influence of different temperatures and vibration loads, the corrosion rates of dolomite and limestone are somewhat different.

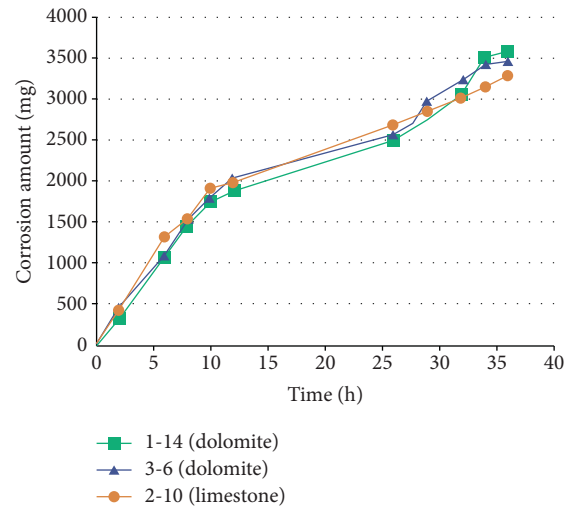

Figure 13: Comparison of corrosion test results of dolomite and limestone under the same conditions.

Temperature is one of the important factors affecting the properties of dolomite and limestone. In fact, the corrosion process of dolomite and limestone is a process in which ions in the lattice of carbonate minerals leave their original positions and transfer into water under the influence of electric charge and thermodynamic conditions of the polar molecules in the erosive water. In the surface environment, this process involves a three-phase complex system of gas, liquid, and solid, and their chemical reactions are influenced

Table 4: List of parameters and corrosion results of limestone and dolomite samples.

Sample no.	Lithology	Weight g	Diameter Mm	Height mm	Surface area mm^2	Volume mm^3	Density g/cm^3	Corrosion amount mg	Corrosion amount per unit area, mg/mm^2
4–7		119.45	68.50	12.26	10003.84	45158.68	2.65	2246.13	0.225
4–14	Limestone	118.14	68.68	12.01	9995.619	44470.63	2.66	3749.75	0.375
4–6		118.17	68.47	12.15	9972.58	44714.32	2.64	4216.24	0.423
1–10		121.90	67.88	12.69	9938.867	45900.24	2.66	2652.67	0.267
1–12	Dolomite	122.08	68.79	12.35	10096.95	45876.18	2.66	2916.88	0.287
1–11		124.48	68.74	12.71	10161.92	47144.85	2.64	4604.62	0.456

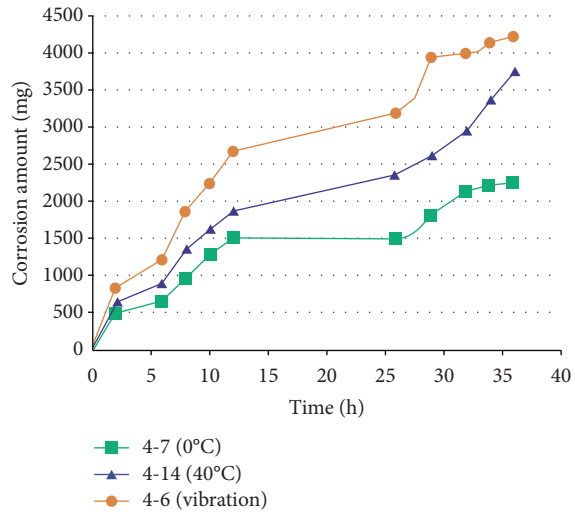

Figure 14: Comparison of the corrosion test results of dolomite under different conditions.

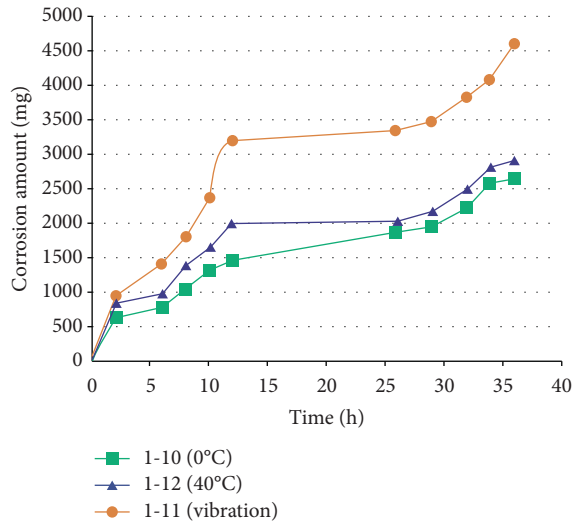

Figure 15: Comparison of the corrosion test results of limestone under different conditions.

by many factors such as pH, temperature, hydrodynamic conditions, specific surface area of minerals, genesis structure of minerals, and external vibration load conditions. In northern Guangxi, the solar radiation is intense, the average sunshine time is long, and the rock surface heats up quickly and cools down slowly, which has a significant heating effect. Rock surface and Earth surface temperature can reflect the water-heat exchange process of Earth surface, which has a certain influence on the corrosion rate of carbonate rocks. In northern Guangxi, the corrosion amount per unit surface area is 0.267 mg/mm^2 for dolomite, and 0.225 mg/mm^2 for limestone at 0°C. The corrosion amount per unit surface area is 0.287 mg/mm^2 for dolomite, and 0.375 mg/mm^2 for limestone at 40°C. The corrosion rate of both dolomite and limestone increases with the increase of the experimental temperature, and the increasing amplitude for limestone is larger than that for dolomite. This is possible because the dolomite has more pores on the surface, mostly has stratification structures, and is easy to form corrosion films and pores on the surface, while the limestone has fine mineral particles (microcrystalline to powder crystalline), has compact structures, and is more conducive to the surface corrosion with the increase of temperature.

Corrosion includes chemical dissolution and mechanical damage, and vibration load is one of the causes of mechanical damage. With the rapid development of the economy and society and the adjustment of national strategy, more and more high-speed railways and highways need to pass through the karst areas in northern Guangxi. In the process of construction and operation, the influence of vibration loads such as vehicles (especially high-speed trains and urban railway transits) is more conducive to increasing the corrosion rate of dolomite and limestone, especially obvious in the districts with better hydrodynamic conditions. The vibration of the train can increase the deformation of the rock mass, especially the deformation of the rock mass with cracks or connected pores. In addition, vibration loads will aggravate the degree of chemical corrosion of water on the rocks, and the coupling of mechanical destruction and chemical corrosion will lead to the generation of secondary minerals and secondary pores in the rocks, which will accelerate the rate of corrosion reaction. The corrosion rate of dolomite in northern Guangxi is increased significantly under the vibration load conditions, which is about 1.75 times that at 0°C. The corrosion rate of limestone also increased significantly, which is about 1.88 times of that at 0°C. Under the action of vibration load, physical disintegration is dominant in the corrosion process of dolomite, and the rock fragments provided by physical disintegration are more conducive to chemical corrosion. In addition, the uniform intercrystalline pores in dolomite are beneficial to the overall corrosion. However, the distribution of fissuring gaps is

extremely uneven when the limestone is stressed, and thus the limestone is easy to form rock cracks and cave systems, which are characterized by obvious differential corrosion.

5. Conclusions

(1) The dolomite in northern Guangxi mainly has a fine crystalline texture and massive structure, and the ratio of CaO/MgO is generally less than 2.2. The dolomite has high purity. The limestone mainly has a powder crystalline texture and massive structure. The ratio of CaO/MgO is generally greater than 10, and the highest ratio can reach about 140. The limestone also has high purity. The content of acid-insoluble matter is low in dolomite but is high in limestone due to the high content of carbonaceous matter.

(2) The corrosion of dolomite and limestone mainly depends on the chemical composition of rocks, the structure of rocks and minerals, the ratio of different mineral components, seepage conditions, and other factors. The difference in corrosion between dolomite and limestone mainly depends on the ratio of CaO/MgO in their chemical composition, and only when the acid insoluble matter exceeds 10% will the corrosion amount be substantially affected.

(3) Under the same external conditions, the corrosion rates of the pure dolomite and the pure limestone are basically the same. The corrosion amount per unit surface area is 0.341 mg for dolomite, and 0.328 mg for limestone. The corrosion amount per unit surface area of dolomite is slightly larger than that of limestone.

(4) The corrosion rates of dolomite and limestone are largely influenced by temperature and vibration load. The corrosion rates of dolomite and limestone are low at 0°C and are increased with the increase of temperature, but the influence of vibration load on corrosion rate is more significant than temperature.

(5) The influence of chemicals, temperature, and other factors on the dissolution of limestone and dolomite were analyzed based on the experiment. The introduction of vibration conditions is a major feature of this paper. The results can provide technical support for the construction, operation, and maintenance of high-speed railways in the karst rocky area of Southwest China. However, due to the limitations of indoor test conditions, the simulated test may be different from the situation. The authors will simulate the actual situation more realistically in future studies [16].

Data Availability

The research data of the paper can be obtained from Zhanfei Gu by e-mail.

Disclosure

A preprint has previously been published [6], and the link is https://www.researchsquare.com/article/rs-942174/v1.pdf.

Conflicts of Interest

The authors have no conflict of interest to disclose.

Authors' Contributions

Zhanfei Gu was responsible for original writing, methodology, and visualization. Zhikui Liu was responsible for supervision and funding.

Acknowledgments

This research was funded by the National Natural Science Foundation of China (Grant no. 41867039), the Foundation of Technical Innovation Center of Mine Geological Environmental Restoration Engineering in Southern Area (Grant no. CXZX 120201002), project funded by Guangxi Key Laboratory of Geotechnical Engineering (20-Y-XT-03), Key R&D and Promotion Projects in Henan Province (Grant no. 222102320177), and project funded by Key Scientific Research Projects of Colleges and Universities in Henan Province (Grant no. 22A560019).

References

[1] P. Liu, G. D. Couples, J. Yao, Z. Huang, W. Song, and J. Ma, "A general method for simulating reactive dissolution in carbonate rocks with arbitrary geometry," *Computational Geosciences*, vol. 22, no. 5, pp. 1187–1201, 2018.

[2] C. b. Zhao, B. Hobbs, and A. Ord, "Effects of different numerical algorithms on simulation of chemical dissolution-front instability in fluid-saturated porous rocks," *Journal of Central South University*, vol. 25, no. 8, pp. 1966–1975, 2018.

[3] C. Zhao, H. Bruce, and O. Alison, "A New Alternative Approach for Investigating Acidization Dissolution Front Propagation in Fluid-Saturated Carbonate Rocks," *Science China Technological Sciences*, vol. 8, pp. 1–14, 2017.

[4] Q. Liu, Y. Lu, and F. Zhang, "Laboratory simulation experiment on dissolution of limestone under hydrodynamic pressure," *Carbonates and Evaporites*, vol. 28, no. 1-2, pp. 3–11, 2013.

[5] Q. Liu, Z. Gu, Y. Lu, and Z. Liu, "The experimental study of dolomite dissolution and pore characteristics in shibing, guizhou," *Acta Geoscientia Sinica*, vol. 36, no. 4, pp. 413–418, 2015.

[6] Z. Gu and Z. Liu, *Experimental study on the structural features and corrosion characteristics of dolomite and limestone in the karst stone mountainous areas in northern Guangxi,* Guangxi, 2022.

[7] M. She, J. F. Shou, A. J. Shen, Y. Zhu, and X. P. Zheng, "Experimental simulation of dissolution for carbonate rocks in organic acid under the conditions from epigenesis to deep burial environments," *Geochimica*, vol. 43, no. 5, pp. 276–286, 2014.

[8] X. H. Wei, T. T. Ma, J. Wang, and H. Z. Ye, "The simulation study of the effect of liquid with different pH values on corrosion for limestone," *Journal of Foshan University (Social Science Edition)*, vol. 31, no. 2, pp. 17–22, 2013.

[9] Z. Guo, Y. Shen, S. Wan, W. Shang, and K. Yu, "Hybrid intelligence-driven medical image recognition for remote patient diagnosis in internet of medical things," *IEEE Journal of Biomedical and Health Informatics*, vol. 1, 2021.

[10] L. X. Zhang, Q. H. Zhao, X. B. Hu, and Z. H. A. O. Xing, "Laboratory dissolution test on dolomite and its micro-dissolution mechanism," *Journal of Engineering Geology*, vol. 20, no. 4, pp. 576–584, 2012.

[11] M. She, Y. M. Jiang, A. P. Hu, and A. Raoof, "The progress and application of dissolution simulation of carbonate rock," *Marine Origin Petroleum Geology*, vol. 25, no. 1, pp. 12–21, 2020.

[12] M. A. Nomeli and A. Riaz, "Effect of CO_2 solubility on dissolution rate of calcite in saline aquifers for temperature range of 50–100 °C and pressures up to 600 bar: alterations of fractures geometry in carbonate rocks by CO_2 acidified brines," *Environmental Earth Sciences*, vol. 76, no. 9, p. 352, 2017.

[13] A. A. Eliwa and A. Atef, "Kinetics and thermodynamics of carbonate dissolution process of uranium from abu-zeniema wet crude uranium concentrates," *Journal of Radioanalytical and Nuclear Chemistry*, vol. 312, no. 1, pp. 1–11, 2017.

[14] M. Mutlutürk, R. Altindag, and G. Türk, "A decay function model for the integrity loss of rock when subjected to recurrent cycles of freezing–thawing and heating–cooling," *International Journal of Rock Mechanics and Mining Sciences*, vol. 41, no. 2, pp. 237–244, 2004.

[15] W. X. Ding, T. Xu, and H. Wang, "Experimental study of mechanical property of limestone under coupled chemical solution and freezing-thawing process," *Yanshilixue Yu Gongcheng Xuebao/chinese Journal of Rock Mechanics & Engineering*, vol. 34, no. 5, pp. 979–985, 2015.

[16] W. Xie, GY. Gao, J. Song, and Y. Wang, "Ground vibration analysis under combined seismic and high-speed train loads," *Underground Space*, vol. 7, no. 3, pp. 363–379, 2021.

[17] M. Vital, D. E. Martínez, N. Borrelli, and S. Quiroga, "Kinetics of dissolution processes in loess-like sediments and carbonate concretions in the southeast of the province of Buenos Aires, Argentina," *Environmental Earth Sciences*, vol. 75, no. 17, p. 1231, 2016.

[18] D. Ma, X. X. Miao, Z. Q. Chen, and X. B. Mao, "Experimental investigation of seepage properties of fractured rocks under different confining pressures," *Rock Mechanics and Rock Engineering*, vol. 46, no. 5, pp. 1135–1144, 2013.

[19] T. Ishibashi, T. P. McGuire, N. Watanabe, N. Tsuchiya, and D. Elsworth, "Permeability evolution in carbonate fractures: competing roles of confining stress and fluid ph," *Water Resources Research*, vol. 49, no. 5, pp. 2828–2842, 2013.

[20] J. Sheng, L. Fengbin, D. Yao, Q. Huang, H. Song, and M. Zhan, "Experimental study of seepage properties in rocks fracture under coupled hydro-mechanochemical process," *Chinese Journal of Rock Mechanics and Engineering*, vol. 31, no. 5, pp. 1016–1025, 2012.

[21] W. Chen, X. Tan, Y. Hongdan, K. Yuan, and L. Shucai, "Advance and review on thermo-hydro-mechanical characteristics of rock mass under condition of low temperature and freeze-thaw cycles," *Yanshilixue Yu Gongcheng Xuebao/Chinese Journal of Rock Mechanics and Engineering*, vol. 30, no. 7, pp. 1318–1336, 2011.

[22] G. Chen, "Ground vibration analysis induced by high-speed train based on in-situ data," *Yanshilixue Yu Gongcheng Xuebao/Chinese Journal of Rock Mechanics and Engineering*, vol. 34, no. 3, pp. 601–611, 2015.

[23] Y. He, L. Nie, T. Guo, K. Kaur, M. M. Hassan, and K. Yu, "A NOMA-enabled framework for relay deployment and network optimization in double-layer airborne access VANETs," *IEEE Transactions on Intelligent Transportation Systems*, vol. 2021, Article ID 3139888, 15 pages, 2022.

[24] Y. M. Zhu, *Sedimentary Rocks*, pp. 182-183, Petroleum industry publishing house, Beijing, 2008.

[25] Y. Peng, A. Jolfaei, and K. Yu, "A novel real-time deterministic scheduling mechanism in industrial cyber-physical systems for energy internet," *IEEE Transactions on Industrial Informatics*, vol. 18, no. 8, pp. 5670–5680, 2022.